



HAL
open science

Transient conduction heat transfer simulation of a fuel heater

Arlindo T Souza Netto, Arthur V.S Oliveira, Michel Gradeck, Rogério Gonçalves dos Santos

► **To cite this version:**

Arlindo T Souza Netto, Arthur V.S Oliveira, Michel Gradeck, Rogério Gonçalves dos Santos. Transient conduction heat transfer simulation of a fuel heater. Congrès français de thermique, Université de Reims Champagne Ardenne, May 2023, Reims, France. hal-04415482

HAL Id: hal-04415482

<https://hal.univ-lorraine.fr/hal-04415482v1>

Submitted on 24 Jan 2024

HAL is a multi-disciplinary open access archive for the deposit and dissemination of scientific research documents, whether they are published or not. The documents may come from teaching and research institutions in France or abroad, or from public or private research centers.

L'archive ouverte pluridisciplinaire **HAL**, est destinée au dépôt et à la diffusion de documents scientifiques de niveau recherche, publiés ou non, émanant des établissements d'enseignement et de recherche français ou étrangers, des laboratoires publics ou privés.

Transient conduction heat transfer simulation of a fuel heater

Arlindo T. SOUZA NETTO^{1,2}, Arthur V. S. OLIVEIRA³, Michel GRADECK¹, Rogério GONÇALVES DOS SANTOS²

¹Université de Lorraine, CNRS, LEMTA, Nancy F-54000, France

²University of Campinas, School of Mechanical Engineering, Energy Department, Campinas, Brazil

³University of São Paulo, São Carlos School of Engineering, Mechanical Engineering Department, São Carlos, Brazil

*Corresponding authors: theodoro1@univ-lorraine.fr, michel.gradeck@univ-lorraine.fr

Abstract - The reduction of the pollutant emissions of already consolidated technologies like internal combustion engines is one of the orders of the day. Even though rules have changed in Europe, internal combustion engines will continue in production and operation around the world for a considerable time to come. In view of the international efforts to reduce global warming, the pollutant emission rates of internal combustion engines must be urgently decreased. Several innovative strategies are envisaged to reach this objective. Among them, the flexibilization of fuels based on the use of biofuels, like ethanol and blends of biofuels with fossil fuels, in addition to the technique of fuel heating are of great potential. Along with the improvement of the cold phase performance of internal combustion engines, the heating prior to injection into the cylinders of either bio or fossil fuels, as well as of their mixtures, results in considerable decrease in the pollutant emission rates of gases like carbon oxide and non-burned hydrocarbons. Given the short heating time required as well as the high power input, boiling takes place during the fuel heating process. Thus, it is crucial to know in detail the thermal behavior of the heater structure during this process to ensure a safe working condition. Aiming at this objective, the present work presents transient heat conduction simulations of a commercial fuel heater using the software COMSOL. A heat transfer coefficient curve was applied as a boundary condition as if water was the working fluid. These simulations leading to temperature profile along the heater are qualitatively compared with experimental results using a dedicated experimental bench. The initial transient behavior of the current for a 10 V heating test and also the cooling process of the surface after a super-heating condition of the heater were analyzed. Good similarity of shape was found for the analyzed phenomena.

Nomenclature

ρ	density, kg.m^{-3}	J	current density vector, A.m^{-2}
c_p	specific heat, $\text{J.kg}^{-1}.\text{K}^{-1}$	E	electric field vector, V.m^{-1}
T	temperature, K	n	unit vector
t	time, s	<i>Index and exponent</i>	
Q	heat source, W.m^{-3}	<i>elec</i>	electrical
h	heat transfer coefficient, $\text{W.m}^{-2}.\text{K}^{-1}$	<i>ext</i>	external
k	thermal conductivity, $\text{W.m}^{-1}.\text{K}^{-1}$		

1. Introduction

The reduction of pollutant emissions and the improvement of cold phase performance of internal combustion engines (ICEs) can be achieved by heating the liquid fuel prior to its injection into the cylinders [1, 2]. This technique, which demands a prompt heating time and high power input, culminate in the occurrence of boiling on the surface of the heater. The fuel heating condition that occurs during the phase shortly before the driver starts the engine is a

particularly important condition due to the fact that the heater operates in the fuel rail as a closed system, in the absence of any forced flow. This is the most critical stage of the project from a safety point of view, once it implies the rapid boiling of a small, closed volume of inflammable liquid. Furthermore, the highest emission rates observed throughout the operation of an ICE are commonly observed during the cold-phase of the engine [3, 4, 5], thereby emphasizing the relevance of heating the fuel to a desired temperature in order to decrease pollutant emissions during this stage.

Aiming to better understand the thermal behavior of the heater structure during the fuel heating process, this paper presents a qualitative comparison between transient numerical simulations of the heat conduction using COMSOL software and experimental data. For the simulation, a heat transfer coefficient curve was applied as a boundary condition as if water was the working fluid. An experiment in a water bath was performed in a similar condition of that considered in the simulation. We compared the initial behavior of the electric current acting on the heater and the evolution of the heater surface temperature profile during the cooling process after the heater super-heating.

2. COMSOL simulations

Simulations were performed in the software COMSOL based on an axisymmetric modeling of a commercial fuel heater. The 2D axisymmetric simulations of the current, voltage and temperature distribution maps were all performed by means of the electromagnetic tool and thermal modules in COMSOL Multiphysics package.

2.1. Model geometry and materials

Figure 1 presents the axisymmetric geometry proposed for the heater and based on the heater used in the experiments. The modeling of the materials composing the body of the heater was done according to the approach of cylindrical layers of different materials. In this perspective, the helical wire resistor was assumed to be a hollow cylinder, which is surrounded by magnesium oxide. The remaining, superficial part of the heating part is composed of Inconel. The unheated body of the heater is composed of inner and superficial 304 stainless steel interposed by magnesium oxide, Inconel, and air.

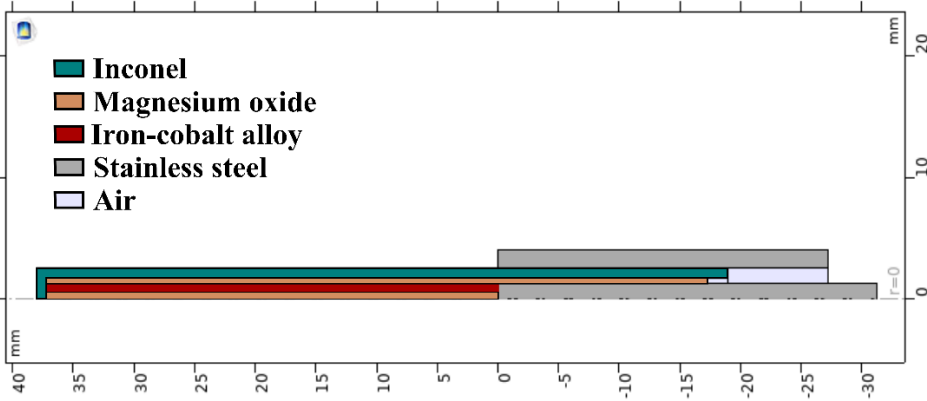


Figure 1: Axisymmetric geometry of the fuel heater.

2.2. Mesh structure

As shown in Figure 2, a free triangular, user-controlled mesh with corner refinement was defined for the entire geometry. Each domain separately meshes with maximum and minimum element size of 0.2 mm and 0.05 mm, respectively. The maximum element growth rate is set to 1.3 with a curvature factor of 0.3. This arrangement resulted in a total of 14502 elements for the mesh.

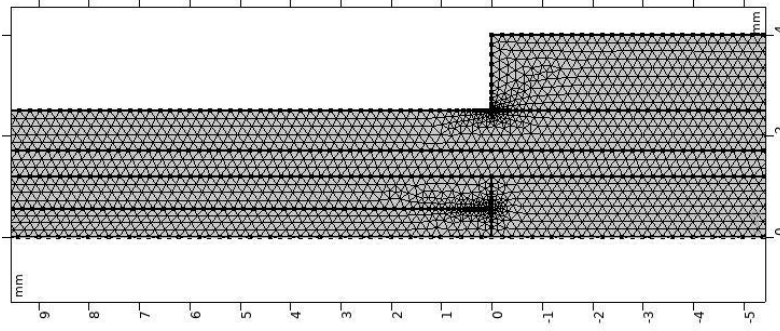


Figure 2: Triangular mesh structure.

2.3. Governing equations

The general heat equation must be solved for the heater solid body and is given by the following partial derivative equation:

$$\rho c_p \frac{\partial T}{\partial t} = -k \nabla^2 T + Q_{elec}$$

where k , c_p and ρ are the thermal conductivity as a function of temperature [W/(m.K)], the specific heat [J/(kg.K)], and the density of the material, respectively. Q_{elec} is the electric heat source term which is given by the dot product of the current density vector and the electric field vector ($Q_{elec} = \mathbf{J} \cdot \mathbf{E}$).

The heat transfer between the heater surface and the water is described by a boundary condition of the third kind:

$$-n \cdot (-k \nabla T) = h(T_{ext} - T)$$

where n is the surface unit normal vector, h is the convection heat transfer coefficient for water at ambient pressure [6] (shown in Fig. 3 as a function of the surface temperature) and T_{ext} is the external fluid temperature.

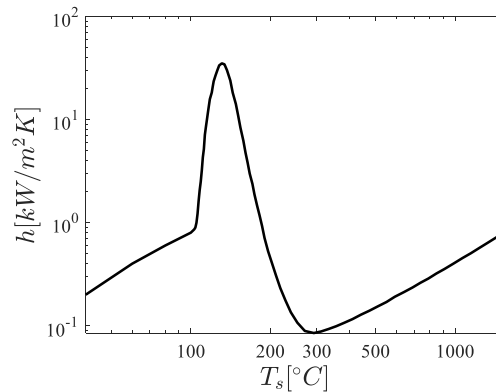


Figure 3: h for water at 1 atm as a function of the surface temperature.

2.4. Electrical and thermal assumptions

The following assumptions were made concerning the electric and thermal boundary conditions:

- The electric potential is applied to the internal steel part of the unheated body (surface marked in red in Fig. 4). The ground is the external steel part of the heater body (surface marked in dark blue in Fig. 4);
- The surface of the heater structure is considered to be electrically insulated (surface marked in yellow in Fig. 4);
- The surface marked in green in Fig. 4 is considered to be thermally insulated;
- The heater is considered to be initially at ambient temperature (20 °C);
- The surrounding fluid temperature (T_{ext}) is considered to be the average between the water saturation temperature (100 °C) and the ambient temperature (20 °C);
- An interpolated boiling curve (shown in Fig. 3) is used as boundary condition at the heater surface (surface marked in yellow in Fig. 4);
- For the super-heating condition simulation, after 6 seconds of heating, a 90% degradation of the HTC is imposed along the central 5 mm of the heated tip surface (region marked in light blue in Fig. 4) for 3 s to represent the transition to film boiling;
- After the end of the heating time, a minimal voltage (100 mV) is supplied to the system until the end of the simulation. This is done because in the experiments this is necessary to continue the acquisition of the electric data.

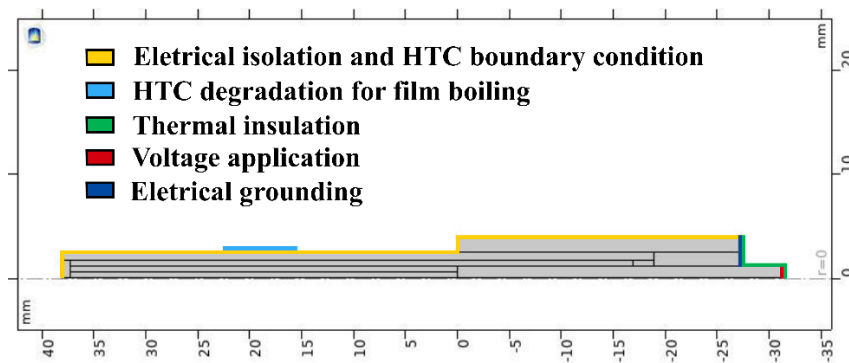


Figure 4: Illustration showing electrical and thermal hypothesis.

3. Experimental apparatus and techniques

As schematically illustrated in Fig. 5, the experimental apparatus consists of a transparent container of dimensions (100×150×100 mm³) filled with water. The fuel heater is allocated horizontally on one side. An acquisition system is used to record the voltage and current data applied to the heater. An infrared (IR) camera with a top view of the experiment provides the infrared images. To ensure accurate measurements with the IR camera, the calibration method proposed by Peña Carrillo et al. [7] was used before the experiments to correlate the heater surface temperature and the digital level measured by the camera. As exposed in [7], this method implies measuring the temperature of the heater surface at a certain axial length of the heated tip with both the IR camera and a K-type thermocouple during a relaxation test. Using this data, a curve is fit to model the temperature as a function of the camera's digital output. The maximum deviation between the model and thermocouple measurements was 5°C, which is considered to be the temperature uncertainty for the IR camera.

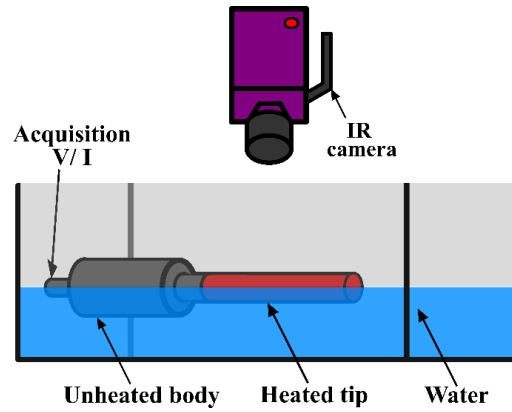


Figure 5: Schematic drawing of the experimental bench.

4. Results and discussion

The first experiment aims to analyze the current drop that occurs at the beginning of a constant tension heating, so the heater was completely submerged in water and a 10 V tension was supplied for 10 seconds. The same parameters were imposed to the simulation. In this test, the heat transfer occurs initially by free convection and afterwards by nucleate boiling, with no transition to film boiling and consequently no super-heating of the heater surface. Figure 6 shows the behavior of the electric tension and current applied to the heater. It is possible to observe a significant immediate drop of the electric current in the first few seconds. The current drop profile observed experimentally is similar to that obtained by the simulation and it happens as a result of the heater resistance rise with the temperature increase (approximately 55% for each 100 °C temperature increase). When the heater reaches a sufficiently high temperature, which is above the saturation temperature, boiling takes place, allowing to verify a stabilization of the current. The current stabilization value differs slightly between the simulation (43.9 A) and the experiment (41.1 A), pointing to the necessity of further investigations concerning the better characterization of the heater and/or of the heat transfer process. This may be related to the possible use of an inappropriate temperature coefficient of resistance for the wire or to inaccuracies of the material properties or of the heat transfer coefficient curve [6] applied as boundary condition. Anyhow, the difference between simulation and test results is very small – about 8% only.

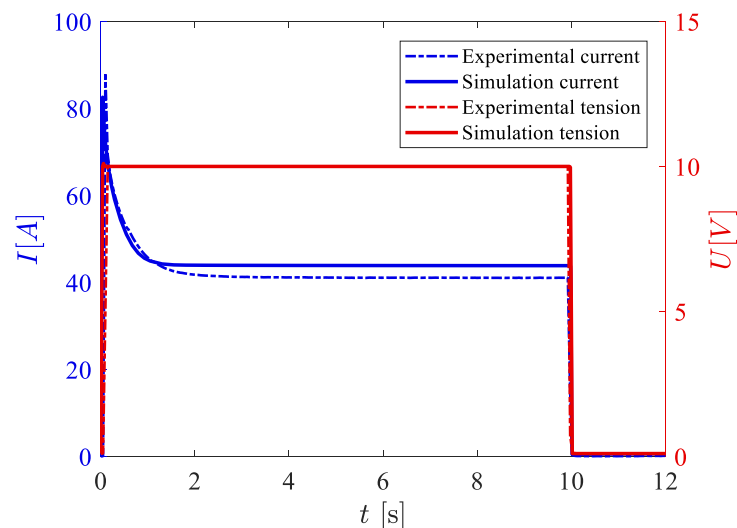


Figure 6: Electrical heating signal for a 10V heating test.

Aiming to compare the surface cooling process observed experimentally and in simulation following a super-heating of the heater, a second experiment is presented. The super-heating is a condition that occurs when a vapor film region is formed on some part of the heater surface. In this scenario, the heat transfer regime transitions from nucleate boiling to film boiling. As a consequence, the heat transfer in such region is degraded and a drastic rise in the surface temperature is observed. For the simulation of this condition, the imposition of the HTC degradation was applied as described in Section 2.3. For the experiment, 10V tension was supplied for a given period of time and manually interrupted when the super-heating of the heater was observed. To enable the IR camera to measure the surface temperature of the heater, the water level in the recipient started just above the symmetry axis of the heater and ended approximately coincident with it. This is not taken into account for the axisymmetric simulations, which consider that the heater is always surrounded by water at T_{ext} . Figure 7 shows the evolution of the heater surface temperature following the super-heating of the central region of the heater and the interruption of the power supply. Regarding the shape of the temperature profile, reasonable similarity can be noticed for the film region. At the tip of the heater, slightly higher temperatures are observed compared to the base, possibly due to a slight misalignment of the heater axis with respect to the water level. Furthermore, it is possible to observe that the cooling occurs faster for the experiment than for the simulation, and it is still necessary to further investigate why this happens.

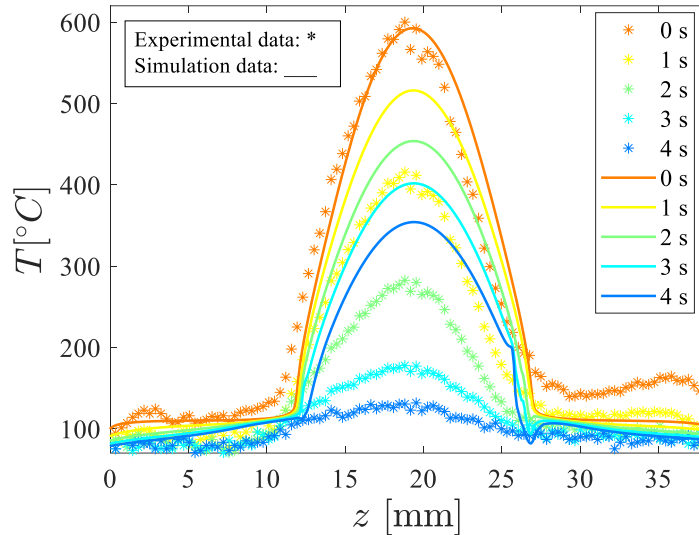


Figure 7: Cooling surface temperature profile evolutions obtained with simulation and experiment.

5. Conclusion

This paper aimed at studying the transient thermal heat conduction observed in the body of a commercial fuel heater and presenting the first experimental and simulation results of the ongoing project. With the objective of comparing axisymmetric simulations with experiments, two different conditions were analyzed. The initial current drop profile was investigated for a 10 V and 10 s heating test, for which the heat transfer happens by free convection and nucleate boiling. Good shape similarity was verified and a slight difference was found for the current stabilization value for the nucleate boiling period. The second comparative analysis focused on the surface temperature profile evolution for a cooling period immediately after a super-heating occurrence at the center region of the heater. Once again, good similarity of the temperature

profile was observed. On the other hand, the experiment had a higher cooling rate than the simulation, which must be further investigated to improve the simulation quantitative results.

References

- [1] Huang, Y., Hong, G., Investigation of the effect of heated ethanol fuel on combustion and emissions of an ethanol direct injection plus gasoline port injection (EDI+ GPI) engine, *Energy Convers. Manag.*, 123 (2016), 338-347.
- [2] Schulz, F., Beyrau, F., The effect of operating parameters on the formation of fuel wall films as a basis for the reduction of engine particulate emissions, *Fuel*, 238 (2019), 375-384.
- [3] Saliba, G., Saleh, R., Zhao, Y., Presto, A. A., Lambe, A. T., Frodin, B., ... Robinson, A. L., Comparison of gasoline direct-injection (GDI) and port fuel injection (PFI) vehicle emissions: emission certification standards, cold-start, secondary organic aerosol formation potential, and potential climate impacts, *Environ. Sci. Technol.*, 51(11) (2017), 6542-6552.
- [4] Du, B., Zhang, L., Geng, Y., Zhang, Y., Xu, H., Xiang, G., Testing and evaluation of cold-start emissions in a real driving emissions test, *Transp. Res. D: Transp. Environ.*, 86 (2020), 102447.
- [5] Yusuf, A. A., Inambao, F. L., Effect of cold start emissions from gasoline-fueled engines of light-duty vehicles at low and high ambient temperatures: Recent trends. *Case Stud. Therm. Eng.*, 14 (2019), 100417.
- [6] Incropera, F. P., DeWitt, D. P., Bergman, T. L., Lavine, A. S. (1996). *Fundamentals of heat and mass transfer* (Vol. 6, pp. 408-409). New York: Wiley.
- [7] Peña Carrillo, J. D., Oliveira, A. V. S., Labergue, A., Glantz, T., Gradeck, M. (2019). Experimental thermal hydraulics study of the blockage ratio effect during the cooling of a vertical tube with an internal steam-droplets flow. *International Journal of Heat and Mass Transfer*, 140, 648-659.

Acknowledgements

This study was financed in part by LEMTA (Université de Lorraine), and by the Coordenação de aperfeiçoamento de Pessoal de Nível Superior – Brasil (CAPES) – Finance Code 001. We also thank the Brazilian federal program ROTA 2030 for the financial support of the construction of the test bench, and Marelli Automotive Systems (Powertrain Division in Hortolândia, Brazil) for providing the fuel heater and its mounting parts for the experiment.